PSFC/JA-03-17

ECCD for Advanced Tokamak Operations Fisch-Boozer versus Ohkawa Methods

J. Decker

September 2003

Plasma Science and Fusion Center
Massachusetts Institute of Technology
Cambridge, MA 02139 U.S.A.

This work was supported by the U.S. Department of Energy, Grant No. DE-FG02-91ER-54109, by the U.S. Department of Energy jointly with the National Spherical Torus Experiment, Grant No. DE-FG02-99ER-54521, and by the U.S. Department of Energy Cooperative Grant No. DE-FC02-99ER54512.

To appear in *Proceedings of the 15th Topical Conference on Radio Frequency Power in Plasmas,* Moran, Wyoming, May 19–21, 2003.

ECCD for Advanced Tokamak Operations Fisch-Boozer versus Ohkawa Methods [1]

Joan Decker

Plasma Science and Fusion Center, MIT, Cambridge MA 02139

Abstract. Current can be driven using electron cyclotron waves (ECW) by optimizing either the Fisch-Boozer mechanism (ECCD) or the Ohkawa mechanism (OKCD). In ECCD, perpendicular heating due to ECW creates an asymmetric resistivity. In OKCD, current is generated by ECW-induced asymmetric electron trapping. OKCD is a good candidate for off-axis CD where the ECCD effectiveness is reduced due to trapped electrons. The two mechanisms are described using the kinetic, bounce-averaged, Fokker-Planck code DKE with a quasilinear ECW operator. Currents and CD efficiencies for the two methods are calculated and compared in different regions of an advanced tokamak plasma. Numerical results confirm the experimental observations that ECCD is best for central CD but becomes ineffective beyond a certain radial distance from the plasma center. On the low-field side (LFS) of this outboard region, OKCD can very effectively generate localized currents. As it is optimized on the LFS, OKCD requires lower wave frequencies than ECCD - an advantage when considering ECW sources.

INTRODUCTION

Electron cyclotron current drive (ECCD) has been successfully used for full current drive [1], current profile control [2], and the stabilization of MHD instabilities, particularly neoclassical tearing modes (NTM) [3][4][5]. In accordance with the Fisch-Boozer method [6], ECW are used to transfer perpendicular energy to the resonant electrons. This creates an asymmetric resistivity, because more energetic electrons are less collisional. This asymmetry in the resistivity generates a electron flow in the same parallel direction as the resonant electron velocity. However, it has been found experimentally [7][1] that the ECCD efficiency decreases as current is driven further off-axis. This decrease in the ECCD efficiency has been understood to be due to the effect of trapped particles. Because ECCD increases the perpendicular energy of electrons, it also diffuses them to a region of velocity space that is closer to the trapped region. A fraction of these electrons are pitch-angle scattered into the trapped region. Since the bounce period of trapped electrons is much shorter than the collisional detrapping time, half of the electron detrapping will occur through the opposite side of the trapped region, thus creating a counter current. The resulting CD efficiency can thus be strongly reduced.

The Ohkawa method [8] for current drive (OKCD) makes use of electron trapping to generate current. The ECW are launched in the opposite direction from ECCD and the wave parameters are chosen so that the wave-particle interaction induces trapping. This trapping

[1] Work carried out in collaboration with Abraham Bers and Abhay K. Ram, *PSFC, MIT*, and Yves Peysson *CEA-Cadarache, France*

creates a depletion of electrons on the resonant side of the velocity space. The fast bounce motion of trapped electrons leads to a symmetric detrapping of electrons. The resulting effect of asymmetric trapping and symmetric detrapping creates a current in the parallel direction opposite from that of resonant electrons.

In the original OKCD description [8] several simplifying and non-self-consistent assumptions were made. Recently, we have shown [9][10] in calculations based upon a complete and self-consistent, neoclassical, 2-D momentum-space Fokker-Planck description of collisions, and quasilinear diffusion due to ECW, that OKCD, with properly chosen ECW frequencies and parallel indices, can effectively generate appreciable currents.

In the following, using our kinetic formulation and code [9][11], we compare ECCD and OKCD in a toroidal geometry. The objective is to determine if the Ohkawa method could be a valuable alternative for far-off axis CD using ECW, where ECCD was found to be ineffective.

KINETIC MODEL

Bounce-Averaged Fokker-Planck Equation

We consider the simplest relevant toroidal geometry in this study of ECCD and OKCD. Toroidal axisymmetry is assumed, and the magnetic flux-surfaces are taken to be circular and concentric.

The steady-state gyro-averaged kinetic equation is given by

$$\mathbf{v}_{\text{gc}} \cdot \nabla f = \mathcal{C}\left(f\right) + \mathcal{Q}\left(f\right) \tag{1}$$

where f is the guiding center distribution function and depends on the 4-D phase-space $f = f\left(r, \theta, p_{\parallel}, p_{\perp}\right)$; r is the radial location and θ is the poloidal angle taken from the outboard horizontal mid-plane. The electron momentum is decomposed into its components $p_{\parallel}$ and $p_{\perp}$ respectively parallel and perpendicular to the magnetic field. $\mathcal{C}$ and $\mathcal{Q}$ are the collisional and RF quasilinear operators respectively. The guiding center velocity $\mathbf{v}_{\text{gc}}$ can be decomposed into the parallel motion along the field lines, and a drift velocity: $\mathbf{v}_{\text{gc}} = \left(\mathbf{v} \cdot \widehat{b}\right)\widehat{b} + \mathbf{v}_{\text{d}}$, where $\widehat{b}$ is the unit vector in the direction of the magnetic field. Usually, in tokamaks, the characteristic times for the parallel motion, collisions and quasilinear diffusion are much shorter than the drift time. Therefore, in first approximation, the drifts can be neglected and electrons are assumed to remain on a given flux-surface. Consequently, the drift-kinetic equation (1) reduces to the Fokker-Planck equation

$$\frac{v_{\parallel}}{r}\frac{B_{\theta}}{B}\frac{\partial f}{\partial \theta} = \mathcal{C}\left(f\right) + \mathcal{Q}\left(f\right) \tag{2}$$

which gives the 3-D distribution function $f = f\left(\theta, p_{\parallel}, p_{\perp}\right)$, and can be solved separately on each flux-surface.

Most tokamaks with reasonably high temperature operate in the low-collisionality regime, or banana regime. In this case, the bounce time τ_b is much shorter that the collisional detrapping time τ_{dt}, so that trapped electrons can perform many bounce periods before being

detrapped. Banana orbits are then well-defined and, to the lowest order in the collisionality parameter, f is constant along the field lines and symmetric in the trapped region. Applying the bounce-averaging operator

$$\{\mathcal{A}\} \equiv \frac{1}{\tau_b}\left[\frac{1}{2}\sum_{\sigma}\right]_T \int_{-\theta_c}^{\theta_c} \frac{d\theta}{2\pi} \frac{r}{\left|v_{\|}\right|} \frac{B}{B_\theta}\mathcal{A} \tag{3}$$

the first term in (2) is annihilated. In (3), θ_c is the turning angle for trapped particles, and the sum over $\sigma = v_{\|}/\left|v_{\|}\right|$ applies only to trapped electrons, for which the average must be performed over both the forward and backward motions. As a result, we obtain the bounce-averaged, Fokker-Planck equation

$$\{\mathcal{C}(f)\} + \{\mathcal{Q}(f)\} = 0 \tag{4}$$

which must be solved numerically in the 2D momentum space.

Numerical Code

Equation (4) is solved using the code DKE [11]. This code uses the fully relativistic collisional operator developed by Braams and Karney [12] and the relativistic RF quasilinear operator proposed by Lerche [13]. Because the distribution function is symmetric in the trapped region, only one half of the trapped region is to be considered in the FP calculations [14]. However, this requires a particular treatment of the particle fluxes in momentum space at the trapped/passing boundary, since electrons that are barely trapped can be detrapped either on the co- or counter-passing side, given that the bounce period is much shorter than the collisional detrapping time. With this scheme, the bounce-averaged dynamics include trapping effects implicitly, leading to very fast computer calculations. In addition, non-uniform grids are used both in momentum and pitch-angle coordinates, allowing for finer calculations in the most important regions of momentum space for ECCD and OKCD, particularly near the trapped/passing boundary.

The calculations presented in this paper were carried out for a typical DIII-D plasma, with major radius $R = 1.67$ m, minor radius $a = 0.67$ m, and magnetic field on axis $B_t = 2.1$ T. The temperature and density profiles were taken to be parabolic, with respective core and edge temperatures $T_{e0} = 4.0$ keV and $T_{ea} = 0.0$ keV, and densities $n_{e0} = 3.0 \times 10^{19}$ m^{-3} and $n_{ea} = 0.4 \times 10^{19}$ m^{-3}. The effective ion charge was taken uniformly $Z_{\text{eff}} = 2$.

The EC wave was considered to be a Gaussian beam of width 2 cm, polarized in the quasi-X mode. The wave-particle interaction occured near the second harmonic, $\omega \simeq 2\Omega_{ce}$.

Moments of the distribution function f calculated from (4) give the flux-surface averaged current density J and the flux-surface averaged absorbed power density p_d. A normalized intrinsic CD figure of merit is defined by

$$\eta = \frac{J/\left(en_e v_{Te}\right)}{p_d/\left(n_e \nu_e m_e v_{Te}^2\right)} \tag{5}$$

where ν_e is the electron collisional frequency $\nu_e = \left(e^2 n_e \ln\Lambda\right)/\left(4\pi\varepsilon_0^2 m_e^2 v_{Te}^3\right)$.

CALCULATIONS ON A SINGLE FLUX-SURFACE

In order to describe the mechanisms of ECCD and OKCD, we first consider a given flux-surface at a normalized radius $\rho \equiv r/a = 0.6$. The EC beam crosses the flux-surface at a poloidal location θ_b. The flux-surface averaged energy flow density incident on the flux-surface is $\langle S_{\text{inc}} \rangle = 230$ kW/m^2. The calculation of ECCD and OKCD depends primarily on the location of the resonance curve in momentum space. This location is given by the resonance condition equation, which can be written as

$$\gamma - N_{\|} \frac{p_{\|}}{mc} - \frac{2\Omega_{ce}}{\omega} = 0 \tag{6}$$

The two relevant wave parameters are therefore the toroidal refractive index $N_{\|}$ and the ratio $2\Omega_{ce}/\omega$. Along the ray path, $N_{\|}$ usually remains relatively constant across the resonance region. Here, we take $N_{\|} = 0.3$ for ECCD and $N_{\|} = -0.3$ for OKCD. However, the variations of $2\Omega_{ce}/\omega$ across the resonance region greatly affect the location of the resonance curve and therefore, the driven current. Considering an EC beam propagating horizontally from the low-field side and crossing the cyclotron resonance near $\rho = 0.6$ with $N_{\|} = \pm 0.3$, we find that the peak of power absorption occurs slightly before the actual resonance, at a value $2\Omega_{ce}/\omega \simeq 0.98$, regardless of the poloidal location θ_b. Therefore, we choose this value, which sets the EC wave frequency.

Two different scenarios are considered. ECCD on the high-field side (HFS) at $\theta_b = 180°$, where trapped particle effects are expected to be minimal, and OKCD on the low-field side (LFS) at $\theta_b = 0°$. The respective 2-D distribution functions are shown on Fig. 1, as well as the "parallel distributions", which are obtained by integration over the perpendicular momentum:

$$F_{\|} = 2\pi \int_0^{\infty} dp_{\perp}\, p_{\perp}\, (f_0 - f_M) \tag{7}$$

ECCD

ECCD is affected by trapped particles even if, on the HFS, no trapped particle directly interacts with the EC wave. In fact, the resonant electrons rapidly move to the LFS where they can exchange momentum with trapped particles. After half a bounce period, which is very short compared to the collisional time scale, these trapped particles can transfer momentum to the counter-passing electrons. This explains the momentum increase of electrons with negative $p_{\|}$, visible on graph (a). It clearly appears as an opposite current on the parallel distribution on graph (c). This counter current reduces the efficiency of ECCD.

The driven current density is $J^{\text{EC}} = 1.7$ MA/m^2 and the density of power absorbed is $p_d^{\text{EC}} = 3.2$ MW/m^3. The figure of merit (5) is then $\eta^{\text{EC}} = 1.8$. For comparison, the current density and figure of merit calculated without including the effect of trapped particles are, respectively, $J_{\text{NT}}^{\text{EC}} = 4.6$ MA/m^2 and $\eta_{\text{NT}}^{\text{EC}} = 3.1$. Thus, even when ECCD is located on the HFS, the trapped particles effect strongly reduces both the driven current density and the ECCD efficiency.

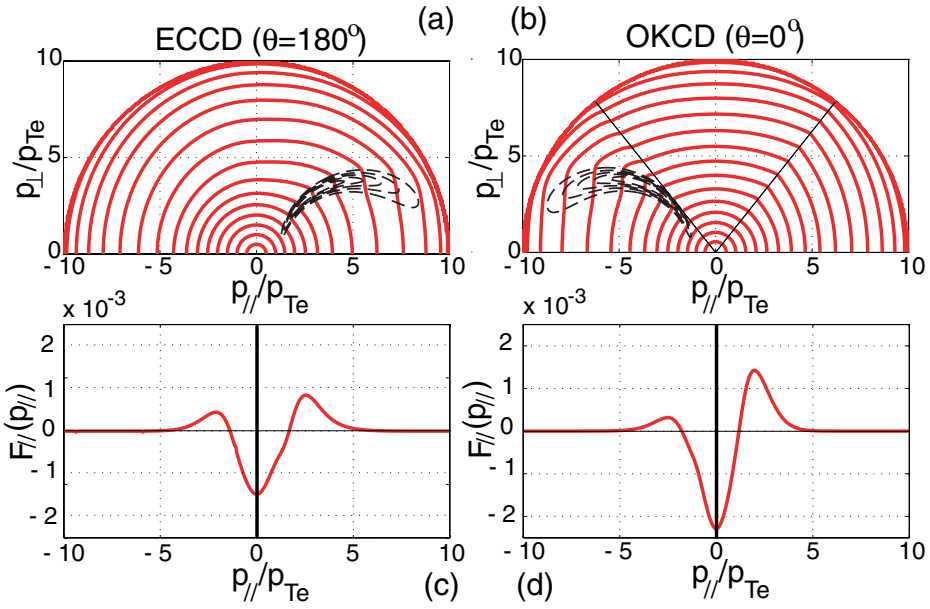

Figure 1: 2D distribution (a)-(b) and corresponding parallel distribution (c)-(d) for the cases of ECCD and OKCD, respectively. The dashed lines on graphs (a)-(b) are a contour plot of the diffusion coefficient. Note that for a Maxwellian, the contours would be equidistant concentric circles.

OKCD

On the LFS, there is a large fraction of trapped particles, so that, in the present case, the resonant region in velocity space -in dashed contours on graph (b)- is located right under the trapped passing boundary. As a consequence, barely counter-passing electrons are trapped under the action of the EC wave, which increases their perpendicular momentum. Because of the fast bounce motion, the distribution function is rapidly symmetrized in the trapped region, and these electrons can be detrapped either on the co- or counter-passing side.

The consequence of an asymmetric trapping due to the wave - which creates a sink of electrons on the counter-passing side -, and the symmetric detrapping, is an accumulation of electrons on the co-passing side. This accumulation is visible on the parallel distribution, shown on graph (d), and generates the Ohkawa current.

The OKCD driven current density is $J^{\mathrm{OK}} = 3.4$ MA/m^2 and the density of power absorbed is $p_d^{\mathrm{OK}} = 6.0$ MW/m^3. The figure of merit (5) is then $\eta^{\mathrm{OK}} = 1.9$. The current density driven by OKCD is sensibly larger than ECCD; however, the density of power absorbed is also larger, so that the figures of merit are comparable. This comparison does not predict how much total current would be driven by a EC beam using the EC or the OK method; however, the larger power absorbed and current densities suggest that OKCD may lead to narrower current profiles, which is important for the accuracy of current profile control and NTM stabilization.

GLOBAL CALCULATION

The distinction between the Fisch-Boozer and Ohkawa effects, which determines the driven current, depends primarily on the location of the wave-particle interaction in momentum space, which varies along the ECW propagation path. Therefore, in order to compare ECCD and OKCD, it is necessary to integrate the total driven current and power absorbed along this path.

OKCD profiles

We consider a ECW launched horizontally, in the mid-plane, from the LFS. Three different OKCD current density profiles are shown on Fig. 2. The radial locations of current deposition were set to $\rho = 0.5/0.6/0.7$, by appropriately choosing the ECW frequency. On the profile centered around $\rho = 0.5$, some negative current is generated first along the ray path, which means that the Fisch-Boozer effect dominates there, because the EC diffusion region in momentum space is far from the trapped region. Closer to the resonance, the Ohkawa effect start to dominate and positive current is driven, because the EC diffusion region in momentum space is near the trapped region. The Fisch-Boozer, negative current decreases if current is driven further off-axis ($\rho = 0.6$) where the fraction of trapped electrons increases; at some point, it becomes negligible ($\rho = 0.7$). This leads to a significant increase in the OKCD current, which is almost twice higher at $\rho = 0.6$ than at $\rho = 0.5$.

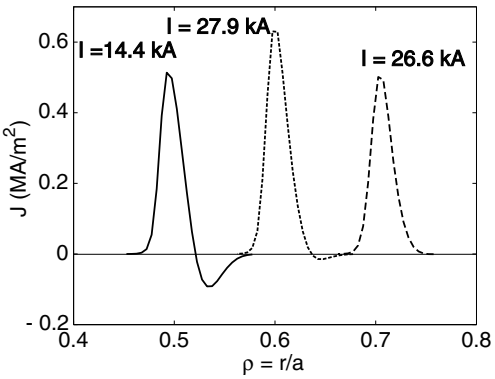

Figure 2: Current density profiles for OKCD at three different radial locations. The total driven current is also indicated. For each case, a beam input power of $P_{\text{inc}} = 1.5$ MW was completely absorbed.

ECCD versus OKCD

In order to compare ECCD and OKCD, we compare the following cases: ECCD on the HFS ($\theta = 180°$), ECCD above the magnetic axis ($\theta = 90°$), and OKCD on the LFS ($\theta = 0°$). The radial location of deposition is modified by varying the EC wave frequency (for $\theta = 0°$ and $\theta = 180°$) or the vertical launching position (for $\theta = 90°$). The ECW is launched with an input power $P_{\text{inc}} = 1.5$ MW and a toroidal launching angle chosen such that $N_{\|} = 0.3$ (ECCD) or $N_{\|} = -0.3$ (OKCD) at the location of deposition. The total driven current is plotted on Fig 3 as a function of the normalized radius.

We can see that the ECCD current decreases steadily with the normalized radius. The decrease is faster for ECCD above the magnetic axis ($\theta = 90°$), which becomes impossible beyond a certain radius ($\rho > 0.6$), in accordance with experimental observations [7]. OKCD current can be driven when the number of trapped particles becomes sufficient ($\rho > 0.4$) and becomes rapidly larger than ECCD at $\theta = 90°$. Beyond some point ($\rho > 0.6$), it becomes even larger than ECCD at $\theta = 180°$. It is interesting to note that, in the present case, OKCD would drive as much current at $\rho = 0.6$ or 0.7 as ECCD at $\theta = 90°$ would drive at $\rho = 0.4$; therefore, OKCD can drive appreciable currents far off-axis, where ECCD cannot. When compared to ECCD at $\theta = 180°$, OKCD gives slightly higher currents for $\rho \geq 0.6$.

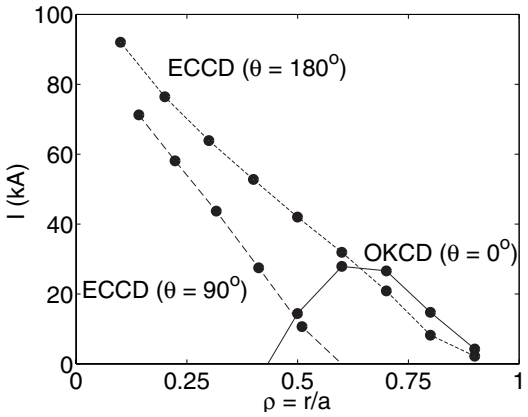

Figure 3: Total current generated by a EC beam of $P_{\text{inc}} = 1.5$ MW launched horizontally from the LFS. Two ECCD cases are considered, with deposition at $\theta = 180°$ or $\theta = 90°$, and a OKCD case at $\theta = 0°$.

Varying the Radial Location of Deposition in OKCD

In ECCD and OKCD, the current is deposited near the intersection of the ray path with the cyclotron resonance layer. Experimentally, the radial location of deposition may have to be controlled and modified during the operation. This has been done by changing the location of the resonance layer, by moving the plasma, or changing the magnetic field [4][3]; it has also been done by steering launching mirrors, in order to modify the ray path [5].

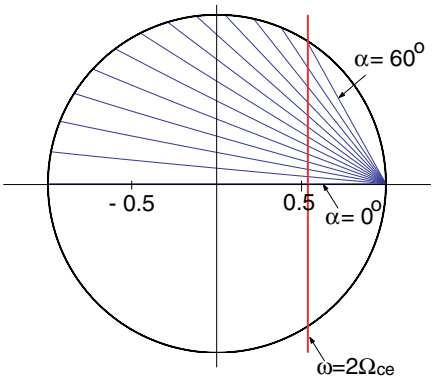

Figure 4: Simulation of OKCD with varying poloidal launching angle. The resonance layer is maintained fixed.

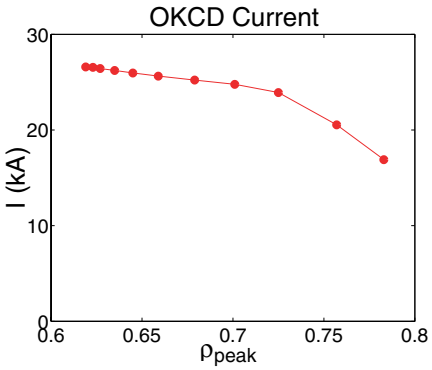

Figure 5: OKCD total current as a function of the current profile peak ρ

The effect of steering the poloidal launching angle is investigated by calculating OKCD with launching from the LFS at an angle α with respect to the horizontal plane. The ECW frequency, and therefore the resonance layer, is fixed, as shown on Fig. 4. The EC beam

input power is $P_{\text{inc}} = 1.5$ MW, and the toroidal launching angle is $\phi = -15°$, so that the parallel refractive index at the location of deposition varies from $N_{\|} \simeq -0.3$ for $\alpha = 0$ to $N_{\|} \simeq -0.2$ for $\alpha = 50°$.

The total driven OKCD current is calculated, and shown on Fig. 5 as a function of the radial location of the current profile peak. The current decreases with ρ, but not as fast as in the case where the radial location is modified by changing the location of the resonance layer (Fig. 3). In fact, the driven current does not vary much over a radial range larger than 10% of the plasma, making OKCD compatible with a steering manipulation for controlling the current deposition location.

CONCLUSION

Experiments have shown that ECCD, effective close to the core, becomes very ineffective or even impossible when driven far off-axis. In this paper, we have shown that in this region, of interest to advanced tokamak operation scenarios, OKCD can offer a valuable alternative, as it drives current with reasonable figures of merit over a large range of far off-axis locations.

ACKNOWLEDGMENTS

Work supported by U.S. DoE Grants DE-FG02-91ER-54109 and DE-FG02-99ER-54521, and Cooperative Grant No. DE-FC02-99ER54512.

References

[1] Sauter, O., et al., *Phys. Rev. Lett.*, **84**, 3322-3325 (2000).

[2] Murakami, M., et al., *Phys. Plasmas*, **10**, 1691-1697 (2003).

[3] Gantenbein, G., et al., *Phys. Rev. Lett.*, **85**, 1242-1245 (2000).

[4] La Haye, R.J., et al., *Phys. Plasmas*, **9**, 2051-2060 (2002).

[5] Isayama, A., et al., *Plasmas Phys. and Cont. Fusion*, **42**, L37 (2001).

[6] Fisch, N.J., and Boozer, A.H., *Phys. Rev. Lett.*, **45**, 720-722 (1980).

[7] Petty, C.C., et al., *Nuclear Fusion*, **41**, 551-565 (2001).

[8] Ohkawa, T., *General Atomic Report* no. 4356.007.001 (1976).

[9] Decker, J., Peysson, Y., Bers, A., and Ram, A.K., "Self-consistent ECCD calculations with bootstrap current", in *Proc. EC-12 Conference*, Aix-en-Provence, France (2002).

[10] Decker, J., Peysson, Y., Bers, A., and Ram, A.K., "On Synergism between Boostrap and Radio-Frequency Driven Currents", in *29th EPS Conference on Plasma Phys. and Cont. Fusion*, Montreux, Switzerland (2002).

[11] Peysson, Y., Decker, J., and Harvey, R.W., "Advanced 3-D Electron Fokker-Planck Transport Calculations", in *AIP Proc. RF- 15 Conference*, Moran, WY (2003).

[12] Braams, B.J., and Karney, C.F.F, *Phys. Fluids B*, **1**, 1355-1368 (1989).

[13] Lerche, I., *Phys. Fluids*, **11**, 1720-1726 (1968).

[14] Killeen, J., et al., *Computational Methods for Kinetic Models of Magnetically Confined Plasmas*, Springer-Verlag, 1986.